Acta Biomaterialia 14 (2015) 154–163

Contents lists available at ScienceDirect

Acta Biomaterialia

journal homepage: www.elsevier.com/locate/actabiomat

Temperature effects on the fracture resistance of scales from *Cyprinus carpio*

Sandra Murcia [a], Mikaela McConville [b], Guihua Li [c], Alex Ossa [d], D. Arola [a,*]

[a] Department of Materials Science and Engineering, University of Washington, Seattle, WA, USA
[b] Department of Mechanical Engineering, University of Maryland Baltimore County, Baltimore, MD, USA
[c] School of Electrical Engineering and Automation, Anhui University, Hefei, China
[d] School of Engineering, Eafit University, Medellín, Colombia

ARTICLE INFO

Article history:
Received 23 August 2014
Received in revised form 30 October 2014
Accepted 18 November 2014
Available online 4 December 2014

Keywords:
Elasmoid scales
Tear test
Fracture resistance
Microstructure
Anatomical position

ABSTRACT

In this investigation the fracture resistance of scales from *Cyprinus carpio* was evaluated as a function of environmental temperature. Tear specimens were prepared from scales obtained from three characteristic regions (i.e. head, mid-length and tail) of multiple fish. The fracture resistance was characterized in Mode III loading and over temperatures ranging from −150 °C to 21 °C. Results showed that there was a significant reduction in tear resistance with decreasing temperature and the lowest resistance to fracture was obtained at −150 °C. There was a significant difference in the relative tear toughness between scales from the three locations at ambient conditions (21 °C), but not below freezing. Scales obtained near the head exhibited the largest resistance to fracture (energy ≈ 150 ± 25 kJ m^{-2}) overall. The fracture resistance was found to be primarily dependent on the thickness of the external mineralized layer and the number of external elasmodine plies, indicating that both the anatomical position and the corresponding microstructure are important to the mechanical behavior of elasmoid fish scales. These variables may be exploited in the design of bioinspired armors and should be considered in future studies concerning the mechanical behavior of these interesting natural materials.

1. Introduction

Nature has served to inspire solutions to technical problems in many areas of engineering. While no longer new, the field of bioinspiration is contributing to the design and development of novel materials with exceptional properties (e.g. Refs. [1–8]). Over the past decade the search for more advanced structural materials has extended to animals with "armored skins", like those possessed by armadillos, crocodiles, turtles and fish. The architecture of the aforementioned natural armors differs according to the pattern of assembly, the way the hard platelets are embedded within the skin and their unique hierarchical structures [9]. For example, the scales in fish are distributed along the body, overlapping such that the posterior region of a single scale covers a portion of both adjacent lateral and posterior scales. This staggered arrangement endows fish with a combination of protection from physical attack and essential flexibility for locomotion [10].

The scales in modern fish are classified into four groups, including cosmoid, placoid, ganoid and elasmoid [10,11]. Placoid scales of sharks have been studied for hydrodynamic purposes [12]. Ganoid scales, known as bony scales, exhibit a microstructure similar to that of bone [11,13–16] and can be found in the alligator gar. The microstructure of ganoid scales can be divided into two main layers. The outer ganoine layer consists of apatite crystals (similar to tooth enamel) and the inner bone basal layer is largely constructed of mineralized type I collagen fibers [15]. The mechanical properties of ganoid scales have been characterized from different teleosts, including the alligator gar (*Atractosteus spatula*) [15–17] and *Polypterus senegalus* [8,13,14]. Nanoindentation tests performed on ganoid scales have shown that both the modulus and hardness exhibit spatial variations through the thickness, which appears related to the distribution of mineral [14–16]. Yang et al. [17] characterized the tensile and compressive properties of the alligator gar scales, and found that the scales exhibit inelastic behavior when hydrated. The investigators also evaluated the fracture resistance of scales from the alligator gar via three-point bending in situ within an electron microscope. According to fracture resistance curves, the fracture toughness of the tissue ranges from 2.5 to 6 MPa m$^{1/2}$, which is comparable to that of other mineralized tissues such as bone and dentin [18].

While the segmented assembly of ganoid scales bestows a degree of flexibility, single scales are far less compliant. This is not ideal for body armors that may require unrestricted movement.

* Corresponding author. Tel.: +1 206 685 8158; fax: +1 206 543 3100.
E-mail address: darola@u.washington.edu (D. Arola).

http://dx.doi.org/10.1016/j.actbio.2014.11.034
1742-7061/

In contrast, elasmoid scales are flexible. They are also composed of two primary layers. The external layer is highly mineralized and composed of calcium-deficient apatite or calcium carbonate, depending on the fish [15,19]. The internal layer is a composite of minerals and type I collagen fibers organized in unique plies that are arranged in the form of a plywood structure. The diameter of the collagen fibers is ~1 μm, and they are constructed of an assembly of fibrils ~100 nm in diameter [19–25]. Individual fibrils and interfibrillar minerals have been observed in evaluations performed with transmission electron microscopy (TEM) and atomic force microscopy (AFM) [15,19,25].

Interesting studies have been performed on the mechanical properties of elasmoid scales from the *Pagrus major* [20], *Arapaima gigas* [22,25,26], striped bass (*Morone saxatilis*) [24,27] and carp (*Cyprinus carpio*) [19]. Ikoma et al. [20] evaluated the tensile properties of dehydrated scales of *Pagrus major* and reported an elastic modulus and tensile strength of 2.2 ± 0.3 GPa and 93 ± 1.8 MPa, respectively. Scales of *Arapaima gigas* in the hydrated condition showed an elastic modulus of 0.8 ± 0.1 and tensile strength of 22.3 ± 3.9 MPa; these values increased to 1.4 ± 0.2 GPa and 53.9 ± 8.4 MPa, respectively, with dehydration [25]. An evaluation using nanoindentation showed a reduction in hardness and modulus from the exterior to the interior layers [22,25]. Garrano et al. [19] found that the mechanical behavior of carp scales is a function of hydration and anatomical position; scales from the tail region exhibited significantly lower elastic modulus and strength than those from the mid-length and head regions. Equally important, recent evaluations of scales in uniaxial tension showed evidence of mechanical anisotropy [24,25].

Armors should be strong and resistant to fracture. An ideal armor would be one whose performance is also independent of environmental factors. Currey [28] stated that some fish scales are so tough that they are difficult to tear, even after immersion in liquid nitrogen. That comment suggests that the fracture resistance of these natural armors could be independent of temperature. However, no study has evaluated the importance of temperature on the fracture resistance of fish scales. Therefore, the primary objective of this investigation was to evaluate the fracture resistance of elasmoid fish scales and the importance of temperature for the first time.

2. Materials and methods

Five individual *Cyprinus carpio* fish (i.e. the common freshwater carp) were obtained from a commercial vendor. These fish were marketed as East Asian carp, and no additional information was available for record. Scales were extracted from three regions of the body of each fish after Garrano et al. [19], namely adjacent to the head, from within the mid-length (beneath the dorsal fin) and near the tail (Fig. 1a). The scales were obtained nearly equidistant between the ventral and dorsal aspects of the body. All of the scales were less than 1 mm thick and possessed an effective diameter that depended on the anatomical position. Scales from the head region had an effective diameter (d) equal to or greater than 25 mm. Those obtained from the middle and tail regions ranged between $22 \leqslant d < 25$ mm and $19 \leqslant d < 22$ mm, respectively. After extraction the scales were stored in Hanks balanced salt solution (HBSS) at room temperature and evaluated within 2 weeks of harvest.

Trouser-shaped tear specimens were sectioned from the scales using a specially designed punch and stamping process. Owing to the reported anisotropy of elasmoid scales [24,25], specimens were stamped with respect to the longitudinal axis of the fish at orientations of 0°, 45° and 90° (Fig. 1b). Each sample was stamped from the center of the scale, such that crack extension occurred within the region of uniform thickness (Fig. 1b). After sectioning, the specimens were returned to the HBSS bath at room temperature. A central notch was cut from one edge, which was extended through ~70% of the total specimen length. A scribe line was introduced on the surface of the tear specimens to guide the cutting process. Preliminary tests were conducted to compare the tear resistance of specimens which had notches prepared using a razor blade and a pair of precision-sharpened scissors. Based on measures of the required energy and work to tear, there was no significant difference in the tear response obtained using the two methods of notch preparation. Thus, the notches were prepared using the scissors throughout the remainder of the investigation. Eight samples were prepared from each anatomical position and for each of the three orientations. The specimen measurements (Fig. 1c) were adapted to the scale diameter, maintaining that the aspect ratio of the trouser specimen for tear testing conformed to ASTM standard D1938 [29].

Elasmoid scales undergo appreciable inelastic strain to failure in the hydrated state [15,18,21] and they are quite thin ($t < 1$ mm). They also reportedly exhibit rate-dependent behavior [21]. These factors add substantial complexity to characterizing the fracture resistance as the traditional methods based on linear elastic fracture mechanics are not applicable. The primary form of threat resulting from predator attack is puncture of the scales with a semi-sharp object (i.e. tooth), which promotes a combination of Mode I and Mode III loading. Rivlin and Thomas [30] characterized the fracture toughness of elastomers in Mode III loading by extending Griffith's theory [31] and relating the tear energy to the critical value for crack growth. Thus, Mode III is a relevant loading format. Although analytical solutions for the tearing energy require knowledge of the detailed stress distribution, a simplified approach has been developed for the trousers specimen (Fig. 2) subjected to Mode III loading. Testing of the specimen is achieved by pulling the two legs out of plane by equal forces and in opposite directions. The tear energy in this configuration can be estimated according to:

$$T = \frac{2\lambda P}{t} - 2bw \tag{1}$$

where P is the tearing force, λ is the extension ratio of the legs, t is the specimen thickness, b is width of the legs and w is the strain energy density in the legs. If the deformation in the specimen legs is negligible in comparison to the displacement corresponding to tearing ($\lambda = 1$ and $w = 0$), then the tear energy is simply described by:

$$T = \frac{2P}{t} \tag{2}$$

According to the relatively large compliance of hydrated fish scales, the assumptions associated with characterizing the tear behavior of elastomers apply to elasmoid fish scales as well. Experimental measurements in rubber showed that when crack propagation is expressed in terms of the tear energy, the relation is independent of specimen type and geometry [30–36].

Tear testing of the specimens was performed under displacement control loading using a universal testing machine (Instron ElectroPuls E1000). The instrument was equipped with a load cell having a full-scale range of 250 N and a load precision of 0.01%. To assure minimum elongation of the legs with respect to the rest of the specimen, 80–90% of the legs were clamped within the compression grips during the experiments. Preliminary experiments were conducted with scales of the head region using stroke rates of 25, 100 and 175 mm min^{-1} to identify potential rate dependence.

The tear energy of the scales in each of the three regions was evaluated as a function of temperature. To maintain the specimen hydration and achieve a desired temperature the specimens were

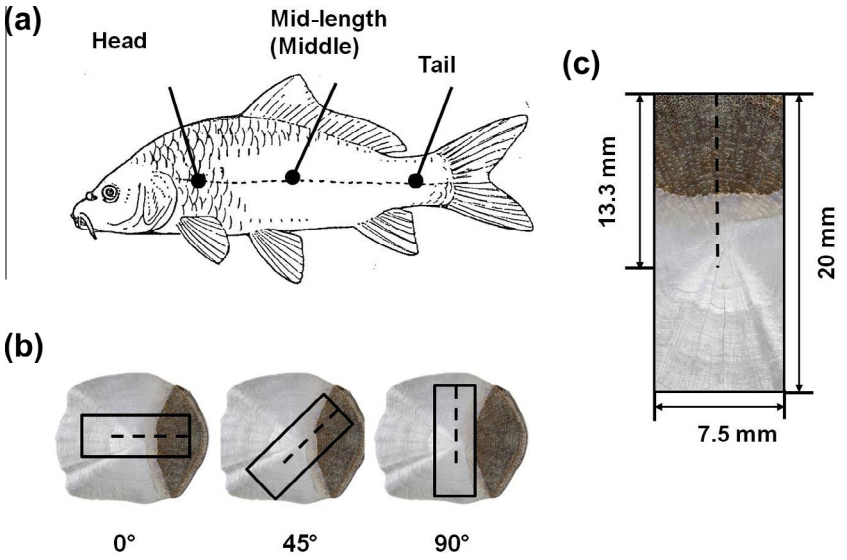

Fig. 1. Details regarding the preparation and characterization of the specimens. (a) Scale extraction according to anatomical position [18], (b) extracted scale showing the three specimen orientations examined with respect to the longitudinal axis of the fish and (c) the rectangular specimen dimensions used for development of the tear specimens.

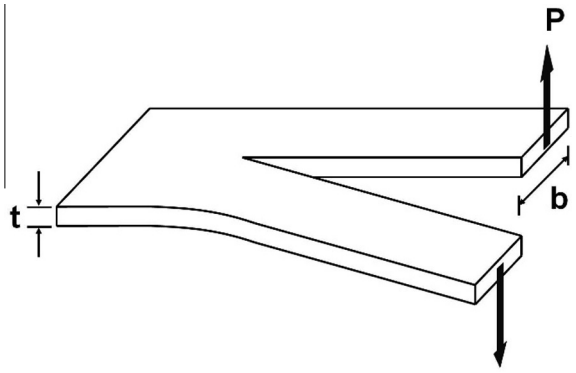

Fig. 2. Schematic diagram of the trouser specimen used for tear testing and definition of variables.

submerged in specific liquid environments while testing. Separate experiments were performed at 21 °C (room temperature), 0 °C, −30 °C and −150 °C using submersion media of HBSS, ice water, dry ice within ethyl acetate and liquid nitrogen, respectively. Specimens of extruded polypropylene (PP) were also evaluated in the aforementioned conditions and used as a control material. These tests were performed at a stroke rate of 250 mm min^{-1}, as recommended by ASTM D1938 for polymers [29]. The glass transition temperature for PP is −10 °C [37]. To dismiss any possible interactions between the polymers or fish scales and ethyl acetate, pilot tests were performed at room temperature after increasing periods of submersion. It was identified that immersion in ethyl acetate had no significant effect ($p > 0.05$) on the tear responses up to ~1 h of exposure. That was substantially longer than the time required for completing the tear tests (less than 1 min).

The energy required to tear the fish scales was estimated from the force–displacement curves of each specimen. The maximum force was identified from the tear history and used with Eq. (2) to estimate the required tear energy. The work required for fracture of the fish scales was also quantified by integrating the area under the force–displacement curves as a function of the tear displacement. For each fish evaluated, eight specimens were tested for each unique parametric condition, with one specimen obtained from each scale. Apparent differences in tear energy and tear work attributed to the independent variables were evaluated for statistical significance using a two-way analysis of variance (ANOVA) and Tukey's honestly significant difference test at $\alpha = 0.05$.

An examination of the fish scale microstructure was performed using an Olympus BX51 optical microscope in reflection mode. Samples were taken from each of the three anatomical positions, and sectioned for inspection along the transverse plane, near the central region. The sectioned scales were fixed in resin and polished with sand paper from mesh numbers of 800 to 4000. Final polishing was performed with a diamond liquid suspension of 3 μm, followed by a liquid suspension of 1 μm Al_2O_3. The microstructure was observed over a range of magnification to distinguish and quantify important features. The thickness and number of plies were recorded for the scales obtained from each carp. These measures were used to explore potential correlations between the microstructure and mechanical properties.

3. Results

The influence of stroke rate and specimen orientation on the tear energy of scales from the head region is shown in Fig. 3. There was no significant difference ($p > 0.05$) in the tear responses over the range of stroke rates in any of the three specimen orientations. However, there were subtle differences in the tear characteristics. At the highest stroke rate the tear deviated from the sample center, whereas at the lowest rate delamination of the scale appeared to be more common. Both of these forms of failure resulted in mixed-mode tear conditions. Therefore, a stroke rate of 100 mm min^{-1} was utilized for the remainder of the investigation to maintain consistency in the mode of failure. If the tear deviated from the center of the sample, that result was discarded due to deviation from the Mode III condition [32–37].

A comparison of the tear energy required for fracture of specimens from the head, middle and tail regions is shown in Fig. 4. The responses in this figure were obtained at room temperature and represent results for all three orientations. As evident from the distribution in these results, there are no distinct spatial variations in the tear resistance of scales, except for the specimens with 0° orientation. Scales extracted from the head region required ~30% greater tear energy than that for scales from the middle

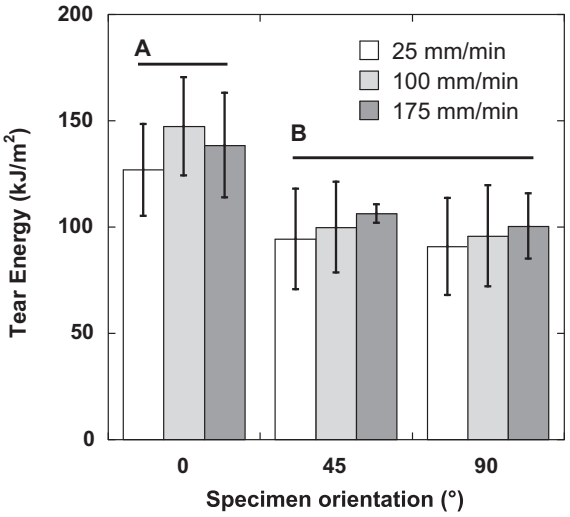

Fig. 3. The importance of stroke rate and specimen orientation on the tear energy. The results in this figure are responses for specimens obtained from scales near the head. Each bar represents the average value along with the standard deviation. Columns with different letters are significantly different ($p \leqslant 0.05$). No significant differences were observed in the tear energy response with stroke rate ($p \geqslant 0.05$).

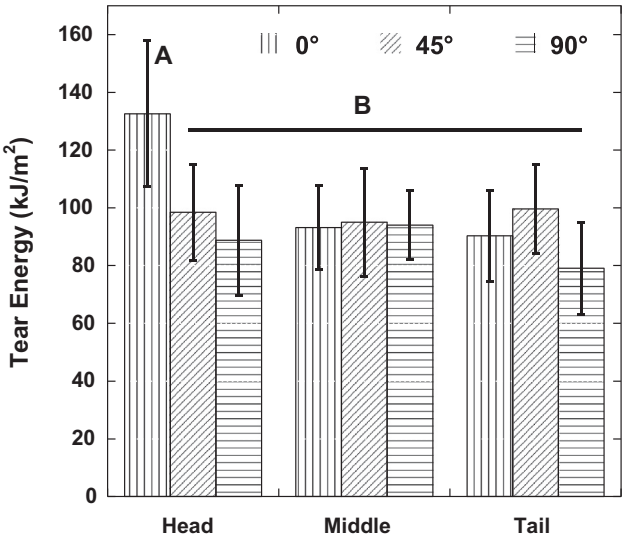

Fig. 4. A comparison of tear energy responses as a function of orientation for scales obtained from the head, middle and tail regions. Results in this figure were obtained at room temperature. Note that the tear energy of head scales with 0° orientation is significantly greater than that over the remainder of the body and other orientations ($p \leqslant 0.01$).

and the tail regions; the differences were significant ($p \leqslant 0.05$). In contrast, the required tear energies for the 45° and 90° orientations were not significantly different ($p > 0.05$) over the three regions of evaluation. Concentrating now on the importance of orientation in Fig. 4, scales from the head exhibited a moderate degree of anisotropy. The tear energy required for fracture in the 0° orientation was significantly greater ($p \leqslant 0.05$) than required for the 45° and 90° orientations. However, scales obtained from within the middle and tail regions did not exhibit anisotropy.

Results from the preliminary testing showed that the 0° orientation exhibited the largest tear resistance (Fig. 3). Furthermore, specimens obtained from scales of the head region possessed the greatest tear resistance of the three regions evaluated (Fig. 4). The influence of temperature on the tear response of specimens from the head region with 0° orientation are shown in Fig. 5a. As

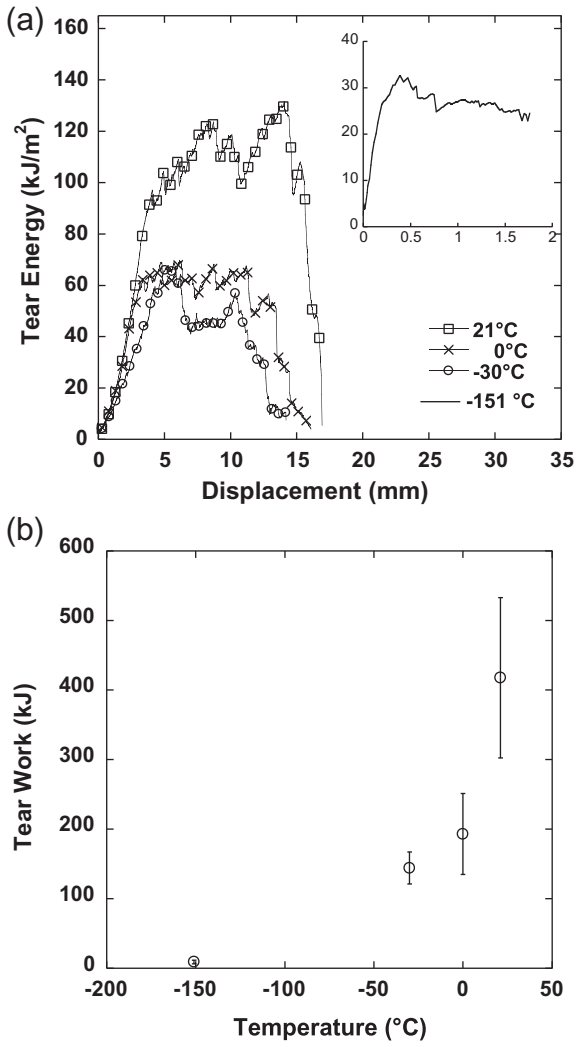

Fig. 5. Fracture resistance of the carp scales and influence of temperature: (a) tear energy vs. displacement for the individual testing temperatures; (b) importance of temperature on the work to fracture. The work to fracture is obtained by integrating the individual tear responses over the tear displacement as shown in (a).

evident in this figure, there is a substantial decrease in tear energy with reduction in temperature. Submersion of the specimens in ice water resulted in a decrease of ~50% in the tear energy with respect to that at room temperature. Both the dry ice and liquid nitrogen environments caused further degradation. The load–line displacement responses were also used to estimate tear resistance in terms of the work to fracture, and the importance of temperature on this measure of resistance is shown in Fig. 5b. It is important to note that the responses in this figure were obtained from scales of the head region and are representative of results obtained from each of the three regions evaluated. Clearly there is a significant decrease in the required work to fracture with decreasing temperature.

The tear resistance of PP was also evaluated as a function of the environmental temperatures to serve as a basis of comparison with the fish scale responses. Preliminary tear tests were conducted with tear oriented parallel and perpendicular to the extrusion direction. Those specimens prepared with parallel orientation underwent uniform Mode III fracture, whereas the samples sectioned perpendicular to the direction of extrusion underwent mixed-mode fracture. Thus, all further evaluation was conducted with tear oriented in the extrusion direction to maintain consistency in the tear mechanics. Typical tear energy vs displacement

curves for the PP specimens at the individual testing temperatures are shown in Fig. 6a. Results for the tear energy measurements at room temperature are in agreement with previous measures [37], thereby validating the method of assessment. At the lower temperatures, fracture of the polymer specimens transitioned from Mode III to a mixed mode response. Mixed-mode tearing was most prominent for the specimens evaluated in liquid nitrogen. In contrast to the responses of the fish scales, there was limited reduction in the energy to fracture with reduction in temperature, except with exposure to liquid nitrogen. Interestingly, there was a distinct reduction in the tear stability at the lower temperatures (Fig. 6a), which is evident in the degree of tear displacement. The influence of temperature on the work to fracture of the PP is shown in Fig. 6b. Similar to results for the scales, there is a significant reduction in the work to fracture over the range in temperatures evaluated.

An overall comparison of the tear resistance for the scales and PP control over the explored temperature range is shown in Fig. 7. Specifically, the fracture energy and work to fracture distributions are shown in Fig. 7a and b, respectively. The density of the carp scales ranges from $\sim 1.10 \pm 0.02$ g cm^{-3} (head) to 0.88 ± 0.03 g cm^{-3} (tail), which is very consistent with that of PP

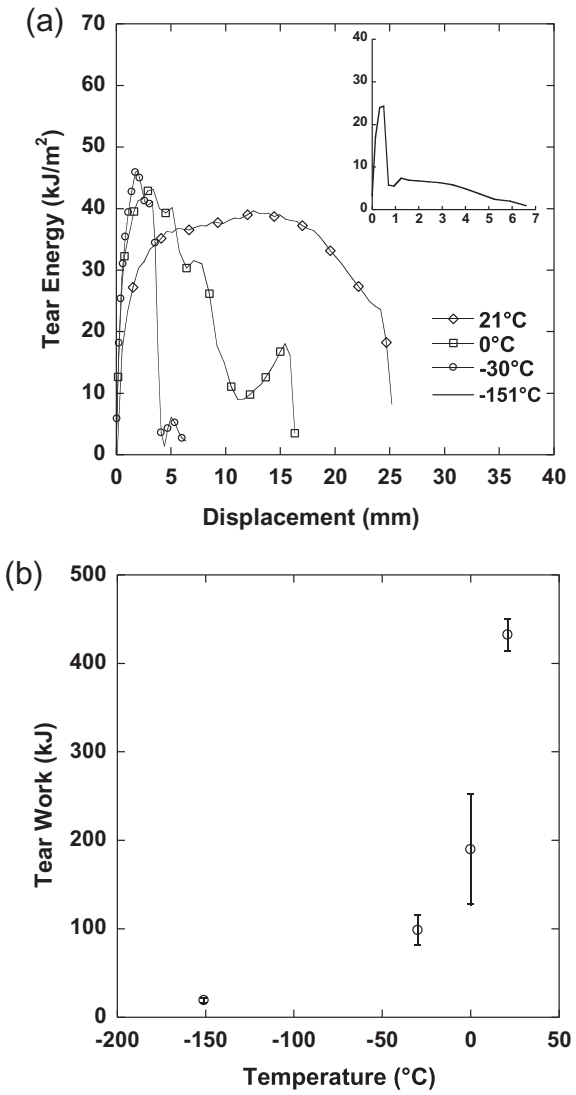

Fig. 6. Fracture resistance of PP and influence of temperature. The orientation of tear was aligned and parallel to the extrusion direction. (a) Change in the tear responses with decreasing temperature; (b) importance of temperature on the work to fracture.

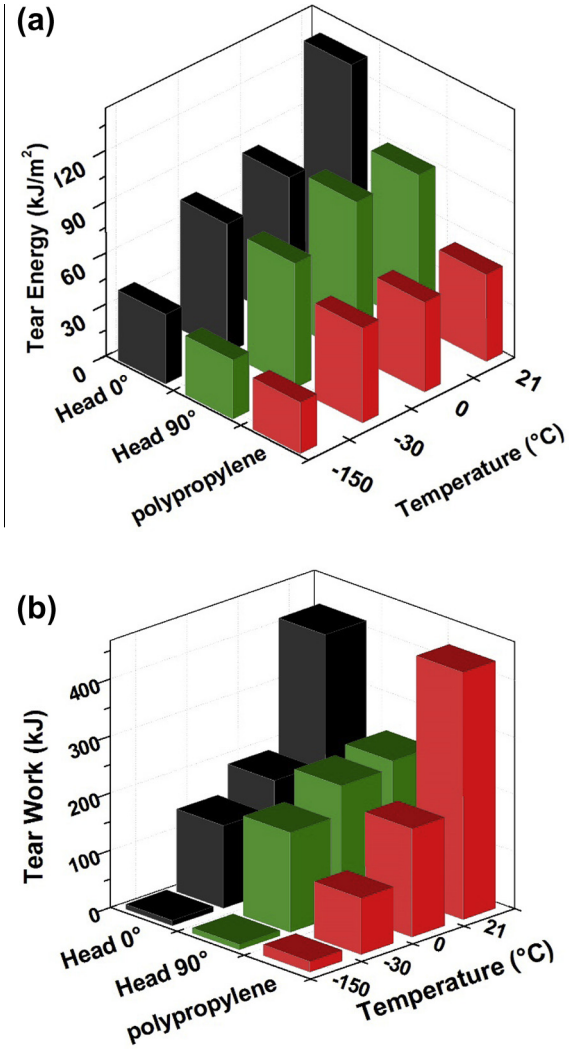

Fig. 7. Comparison of the fracture resistance of carp scales, PP and polystyrene with the influence of temperature. (a) Tear energy results for the carp scales (head region, 0° and 90° orientation) with that of PP and polystyrene. Tear energy of polystyrene is only shown at room temperature since it represents the behavior of the polymer in environments with lower temperatures than its T_g. (b) Tear work results for the carp scales (head region, 0° and 90°orientation) and PP and polystyrene.

(0.95 g cm^{-3}). Hence, the performance ranking in Fig. 7 is the same whether considering the direct measurements or after normalization. At room temperature the carp scales required almost three times more energy to fracture than the PP control (Fig. 7a). While both material systems underwent a significant decrease in tear resistance with reduction of temperature, the fish scales required greater energy to fracture at all temperatures, except after exposure to liquid nitrogen. When evaluated in terms of the work to fracture (Fig. 7b), there is no significant difference ($p > 0.05$) between the performance of the PP control and scales with 0° tear orientation. Although the reduction in temperature was less detrimental to the tear resistance of scales with 90° orientation, there were no significant differences in the tear energy or work of the two orientations, except at room temperature.

Spatial variations in the tear resistance could be attributed to differences in the microstructure between the three regions. The microstructure evident from cross-sections of representative scales from the head, middle and tail regions are shown in Fig. 8a–c, respectively. As evident from these images, the thickness of scales from the three regions are not equal, and scales from the head exhib-

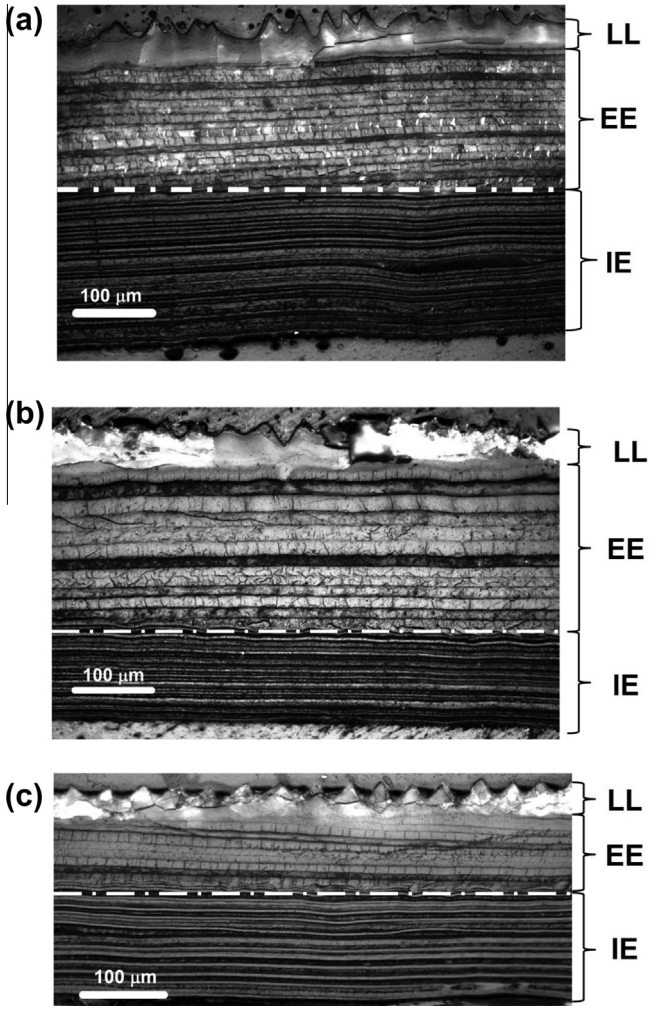

Fig. 8. Cross-section views of sectioned scales and the microstructure within the three regions of evaluation. Representative scales are shown for the: (a) head, (b) middle and (c) tail. The LL is annotated at the top of each micrograph, in addition to the EE and IE regions. The bar represents 100 μm.

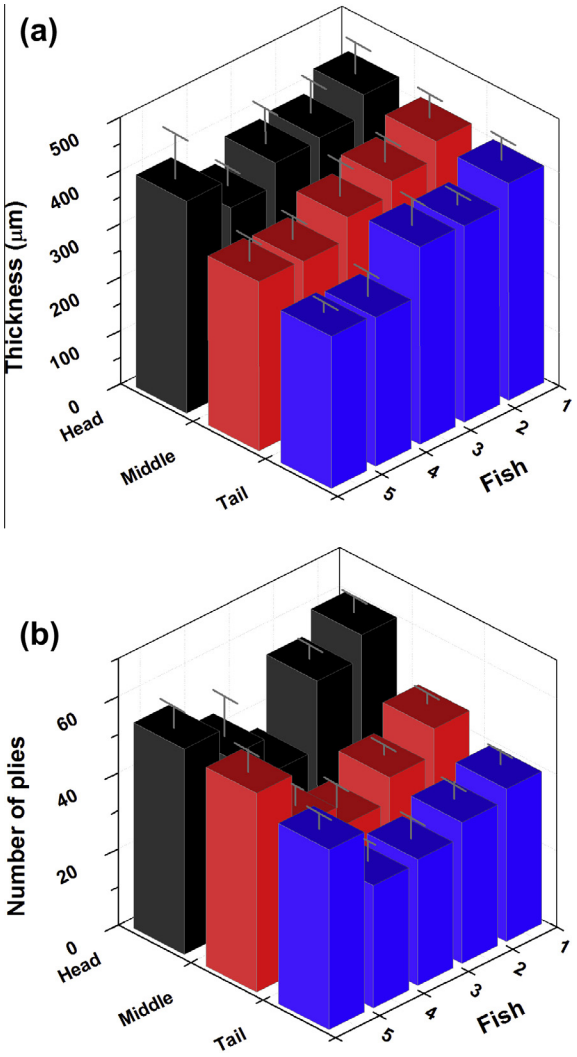

Fig. 9. An analysis of microstructural characteristics of scales obtained from five different fish and within the three regions of evaluation: (a) Scale thickness and (b) total number of plies.

ited the largest thickness overall. Furthermore, the cross-section of each scale can be divided into two distinct layers as annotated in the figures. The most external layer is a highly mineralized "coating" that is referred to as the limiting layer (LL). It is the last part of the scale to develop [38], and promotes a downward diffusion of minerals to the underlying elasmodine layer [39]. The elasmodine is a matrix of type I collagen fibers arranged in plies that can be divided into external and internal sub-layers. The external elasmodine (EE) layer is the first to develop in the process of scale formation, and is followed by the formation of the internal elasmodine (IE). These two sub-layers are quite easy to discriminate in the micrographs presented in Fig. 8, as well as the individual plies within both the EE and IE. Individual plies of the external elasmodine are clearly thicker in comparison to those in the internal layer and are attributed to the higher mineral content [19].

Previous studies on fish scales appear to have incorporated scales from a single fish. As natural materials are not subjected to the same standards of fabrication as those that are engineered, the microstructure of scales from different fish may not be equivalent. Measurements for the total scale thickness and number of plies for the scales of each of the five fish evaluated in this investigation are shown in Fig. 9a and b, respectively. There appears to be a decrease in scale thickness from head to tail in each of the carp evaluated (Fig. 9a). The difference in thickness between the head and tail scales is significant ($p \leqslant 0.05$). However, there was no significant difference in the thickness of scales of the head region amongst the five fish. That is one of the primary reasons for the use of head scales in evaluating the importance of temperature. According to the ply counts, there is a decrease in the total number of plies from the head to the tail (Fig. 9b), and a significantly greater number of plies within scales of the head with respect to the tail ($p \leqslant 0.05$). Interestingly, there are also significant differences in scale thickness and number of plies between the individual fish.

4. Discussion

Fish scales are now serving as inspiration for armor materials [40,41]. Understandably, the majority of scientific efforts in this area have been focused on the puncture resistance. Another key performance requirement of "armors" is resilience to the environmental conditions, including variations in temperature. Fish scales have been purported to be so tough that they are difficult to tear, even after immersion in liquid nitrogen [28]. While it is doubtful that fish would rely on the protective capacity of their scales at temperatures below freezing, the possibility that their construc-

tion bestows them resistance to temperature variations is an exciting prospect.

A comparison of the load–line displacement profiles for the PP (Fig. 6a) shows that there is a reduction in the tear stability with decrease in temperature. Indeed, this is expected as the glass transition temperature of PP is −10 °C [37]. Below that temperature the polymer undergoes embrittlement, which is important to the long-range, coordinated molecular motion that transpires during deformation. At temperatures above the T_g the polymer chains have sufficient thermal energy to move in a coordinated manner (10–50 chains of atoms move). Below that temperature the mobility is substantially restricted (1–4 chains of atoms) [42]. The reduction in polymer chain mobility at temperatures below the T_g suppresses the polymer extensibility and its ability to localize damage in the vicinity of the stress intensity via inelastic deformation. While apparently not critical to the tear energy distribution (Fig. 7a), the in temperature caused substantial degradation to the tear work (Fig. 7b).

Further comparison of the results in Fig. 7 suggests that the mechanisms contributing to changes in the tear resistance of scales with temperature are not equivalent to those operating in the polymer. For instance, the load–line displacement profiles of the scales do not show distinct signs of embrittlement with reduction in temperature. According to the ASTM standard for tear testing [29], that quality is a prerequisite to application of the tear test and in maintaining consistency of the results across the temperature range. In contrast to the polymer, the fish scales undergo reduction in the critical tear force. Of note is that the entire temperature range explored is below the T_g of collagen [43,44]. Temperatures below freezing could change the structure of water molecules residing about the collagen, as well as their interaction with the proteins. In the fracture of brittle or embrittled polymers, inelastic deformation can occur via crazing [42,45]. The crazed zone consists of the development of voids and both extension and rotation of molecular fibrils to an orientation parallel to the maximum normal stress. Yang et al. [25] reported that similar mechanisms contributed to deformation in Mode I fracture of fish scales at room temperature. Dissipation of fracture energy occurred through rotation and stretching of the collagen fibrils as well as via rotation and delamination of the individual plies. This process appears to be a form of crazing, which extends over multiple length scales (fibril and ply). Those plies oriented transverse to the loading direction also undergo distributed delamination, which enables elongation at lower temperatures. Thus, the laminated scale structure appears to result in an apparent lower sensitivity to the decrease in temperature when evaluated by the work to fracture.

In contrast to the control, the scales with 0° orientation underwent a decrease in energy to fracture with reduction in temperature (Fig. 7a), which arises from the changes in critical tear force (Fig. 5a). We believe that the reduction in tear force could result from a diminished participation of the inter-chain hydrogen bonds of the transverse plies at the lower temperature. Alternatively, freezing of the water residing about the collagen could decrease the ability of the fibrils to undergo changes in orientation that would place them in tension, which is more favorable for resisting crack advance [46].

In comparing scales from the three regions, those from the head exhibited significantly greater tear resistance than the other two regions (Fig. 4). Similar findings were reported in the evaluation of the elastic modulus and yield strength of elasmoid scales of carp [19], where the head scales were superior to those from the middle and tail regions. In that investigation the spatial variations were interpreted by ranking the need for protection, i.e. the head and central regions encompass the vital organs of the body, which are more essential to protect. Further explanation stems from the locomotion of swimming, where flexibility of the tail is critical to propulsion of the fish and evasion of attack [47]. But there is a more practical explanation, which comes from the process of scale generation and maturation. Squamation[1] of scales in the carp occurs first in the head region, followed by the middle and then the tail regions [37]. It is essential to add that squamation patterns are not the same in all teleosts and there is some belief that this process is initiated by mechanical stimuli [38]. The squamation chronology of cyprinodontidae shows that there is a lapse of 17 days between the emergences of the first scales in the head to those in the tail [48]. Furthermore, it takes 26 days to fully cover the body of the fish, a time in which differences between head and tail scales could be significant. Indeed, both the scale thickness and number of plies were greatest in scales of the head (Fig. 9). Nevertheless, the differences in tear energy (Fig. 4) were not related to scale thickness as the tear energy accounts for this parameter. Regional differences in scale properties could also be a result of site-specific changes that arise during ontogeny, which influence the collagen distribution and its maturation [39].

In evaluations of engineered composites the number of plies and their orientation are critically important to the mechanical behavior of the laminate (e.g. Refs. [49–51]). Therefore, a relationship between microstructural differences in scales with anatomical position and the mechanical behavior might be expected. Surprisingly, there was no correlation between scale thickness and the tear energy or the tear work. There is a significant difference between the number of plies in scales from the head and the tail ($p \leqslant 0.05$), as shown in Fig. 9b. However, there was also no correlation between the measures of tear resistance and the total number of plies. Therefore, other characteristics should be considered.

Mineralization of fish scales begins once the scale is completely formed and proceeds downward from the limiting layer throughout the life of the fish [23,38,39]. This process results in development of the EE layer, which exhibits thicker plies due to their greater degree of mineralization. A division between the IE and EE layers of the elasmodine can be seen in the micrographs of Fig. 8. The more mineralized portion (EE) was found to exhibit the greatest variation in number of plies with anatomical position. The importance of the number of EE plies on the tear energy distribution is shown in Fig. 10a. As evident in this figure, a larger energy to fracture was required by those specimens with greater number of heavily mineralized plies (i.e. in the EE). The relationship between the internal elasmodine ratio, defining the ratio of IE thickness to total scale thickness, and the work to fracture is shown in Fig. 10b. Overall, there is an increase in the work to fracture with increase in the IE ratio. These results appear to conflict with those of Zhu et al. [24] and Yang et al. [25], who found that the mineralized layers actually reduced the tensile strength of scales from striped bass and *Arapaima gigas*.

The relationships evident in Fig. 10 are akin to those contributing to the performance of many engineered composites. The presence of mineralized layers in the elasmodine is critical to the fracture resistance of the scales. As shown in previous investigations of puncture resistance, the hard mineralized external layer is the first barrier against penetration [24,25,27]. The mineralized layer increases the resistance to local compressive forces, thereby bestowing greater puncture resistance than that of engineering polymers [24]. The ratio of EE and IE in the scale plays an impor-

[1] Squamation is the process of formation of scales in the epidermis of the fish. The establishment of the squamation pattern has been described in several teleost species [39]. In all fish species studied so far, the scales appear very late in ontogeny, i.e., after metamorphosis, when the juveniles are already miniatures of the adults. Usually in the fish skin, cells from which scales start to form, known as fibroblasts, appear only 20–26 days post-fertilization, suggesting that fibroblast invasion requires a specific state of differentiation of the collagen fibrils, and of the cells of the basal epidermal layer.

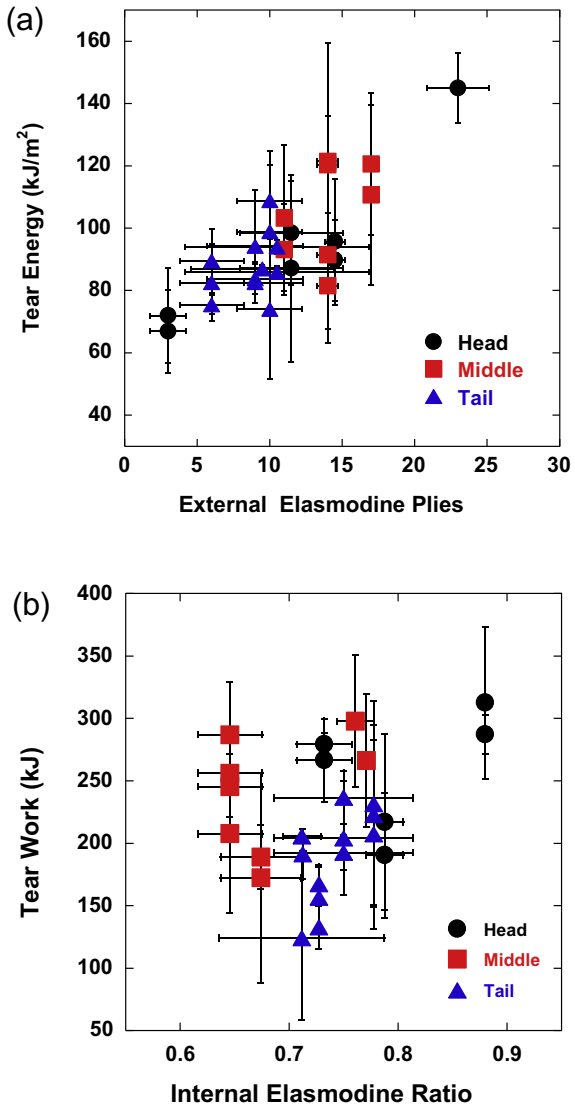

Fig. 10. Relationship between the tear energy and the number of external elasmodine plies: (a) influence of the number of external elasmodine plies and the energy to fracture; (b) influence of the internal elasmodine ratio on the tear work. The internal elasmodine ratio is the ratio of the number of plies in the internal elasmodine and total number of plies in the scale.

tant role as well since the function of the external layers of the EE are to protect the less mineralized layer from direct contact with the penetrating instrument, and to mitigate the stresses transmitted onto the underlying collagen layer by redistributing them over a large area [24]. The primary function of the underlying collagen layers of the IE is in the localization of damage and in preventing its propagation throughout the scale [25]. Considering the tear resistance (Fig. 10b), the IE appears to be essential to the work to fracture and operates to localize damage in the vicinity of the stress intensity.

In the past, the microstructure of teleost scales has been categorized as either a double-twisted [52] or an orthogonal [14–25] plywood structure. Although a detailed analysis of the ply orientations in the carp scales was not conducted, one approach to assess the ply orientations is through the cracking patterns. These are artifacts that develop during dehydration of the scale throughout sample preparation and corresponding non-uniform shrinkage. Yang et al. [17] commented that if every second layer is uncracked, the mis-orientation angle is ~90°; whereas if every third layer is uncracked, this angle is ~60°. Neither of these patterns coincides with the microcracks evident in Fig. 8. The cracks do not appear in every ply, and are most evident within plies of the EE layer. In 2001 Bigi et al. [23] investigated the plywood pattern of collagen fibrils in teleosts with X-ray diffraction (XRD). In their findings, few *Cypriniformes* present a double-twisted plywood structure with an angle of 36°. Moreover, in their study they found a characteristic five orientation pattern of the small-angle XRD reflections on *L. cephalus* scales. This pattern suggests a discontinuous twist of the collagen fibril layers with a 36° rotation from one layer to the following one, resulting in a repetition of orientation every five plies. These discontinuous twists are closer to the observed characteristics of the microcracking patterns. As a definitive description of ply distributions in fish scales has yet to be reported, additional studies aimed at understanding the lamination patterns of scales and their importance to their performance appear warranted.

With all studies there are potential limitations and the present investigation is no exception. Perhaps the greatest concern is related to the use of tear testing for characterizing the fracture resistance. While the primary mode of crack growth in engineering materials and corresponding studies on fracture resistance involve Mode I loading, Mode III fracture is dominant in the puncture of fish scales that results from predator attack. In addition, the scales of carp (elasmoid) are very compliant due to their low mineral content and small thickness, and undergo substantial plastic deformation to failure when hydrated [15,19,22]. Thus, linear elastic fracture mechanics does not apply and an elastic plastic fracture mechanics approach is necessary. However, with the addition of the liquid baths used to achieve the desired environmental temperatures, instrumenting the fracture process to evaluate the near-notch deformation is nearly impossible. There is an additional problem with Mode I loading of fish scales that involves delamination of the scale, which arises from differences in the degree of inelastic deformation exhibited by the different layers [53]. These difficulties were overcome with the Mode III approach and by conducting preliminary studies to identify the appropriate loading parameters. Thus, the tear test provided an effective approach for evaluating fracture resistance that supported a determination of the temperature dependence.

There are legitimate concerns related to application ASTM standard D1938 [29] as a guide for evaluating the fracture resistance of the scales. The low mineral content of the scales and corresponding compliant behavior over the entire range of temperatures roughly conformed to the standard. However, the differences in geometry of scales from the three regions did not completely follow the guidelines. There were variations in the scale thickness, as would be expected for a biological system, with the largest differences noted from scales of middle and tail regions. While the differences in thickness were not directly responsible for the differences in tear energy as evident from Eq. (2), they should be recognized. Additional concerns are related to the specimens used and their preparation. The greatest tear resistance was recorded in the 0° orientation; i.e. with tear proceeding along the longitudinal axis of the fish. With locomotion, the highest bending moment will be experienced in the lateral mid-line of the fish body. This lateral line is where the nerves or neuromats of the fish are located and they are heavily protected with an additional mineral layer [39]. These scales were excluded from the study since they presented prominent deviations in the tear response, including both tear resistance and its orientation. Furthermore, the scales of five different fish were evaluated, with no control for age. As the squamation process and ontogeny of the fish may be important to the microstructure of the scales and its distribution across the body, differences in fish age may have been a contributor to some of the observed variations in mechanical behavior. Another limitation was the potential importance of scale shedding and regeneration to the scales evaluated. It is unknown whether the scales evaluated of any one fish

were original or regenerated. Scale regeneration has been widely studied from a biology perspective [54–56], and would be an exciting scientific pursuit to analyze if there are mechanical differences between old (original) and regenerated scales.

One of the most important findings of the present study is an identification of differences in scale thickness and number of plies within the same species (Fig. 9), and the importance of observed differences in microstructure on the mechanical behavior (Fig. 10). If fish scales will serve to inspire future generations of armor, a better understanding of the relationships between scale design as a laminated system and its contribution to performance is not only relevant, but essential [57,58]. At the very least, the spatial variations in microstructure are important to the mechanical behavior of scales, and there appears to be some important connection with the signals controlling squamation and scale growth. As such, potential spatial variations in scale properties are too easily overlooked and should be considered in future studies of these interesting structural materials.

5. Conclusions

On the basis of results obtained, the following conclusions may be drawn:

1. The microstructure of fish scales is a function of the anatomical position. The total thickness and number of plies in the scales decreased from the head to the tail region. This distribution agrees with the squamation pattern for the *C. carpio*.
2. At room temperature there were spatial variations in the tear resistance of scales obtained from the three characteristic regions evaluated. Those scales obtained from nearest the head required significantly greater energy to tear than those within the mid-length and tail regions. There was no significant difference between the tear energy of scales from the mid-length and tail.
3. There was a significant decrease in the resistance to fracture of the scales with reduction in temperature from ambient conditions to liquid nitrogen environment. Over this range in reduction of temperature there was a 75% decrease in the required work to fracture of the scales overall.
4. Scales obtained from the head region exhibited anisotropy, with the largest tear resistance obtained for tears oriented along the longitudinal direction. Those scales from the other two regions did not exhibit anisotropy. The unique behavior of the head scales appears to be attributed to the larger external elasmodine layer of scales from that region.
5. The tear energy of the scales was found to be strongly related to the number of mineralized plies of the external elasmondine layer. The tear resistance increased with increasing number of elasmodine plies and the total thickness of this layer.

Acknowledgement

This investigation was supported in part by the University of Washington through seed funding (D.A.).

Appendix A. Figures with essential colour discrimination

Certain figures in this article, particularly Figs. 1, 7, 9 and 10, are difficult to interpret in black and white. The full colour images can be found in the on-line version, at http://dx.doi.org/10.1016/j.actbio.2014.11.034.

References

[1] Agnarsson I, Kuntner M, Blackledge TA. Bioprospecting finds the toughest biological material: extraordinary silk from a giant riverine orb spider. PLoS ONE 2010;5(9):e11234.
[2] Li SH, Zeng QY, Xiao YL, Fu SY, Zhou BL. Biomimicry of bamboo bast fiber with engineering composite materials. Mater Sci Eng, C 1995;3(2):125–30.
[3] Mayer G. New classes of tough composite materials—lessons from natural rigid biological systems. Mater Sci Eng, C 2006;26(8):1261–8.
[4] Murphy WL, Mooney DJ. Molecular-scale biomimicry. Nat Biotechnol 2002;20(1):30–1.
[5] Reed EJ, Klumb L, Koobatian M, Viney C. Biomimicry as a route to new materials: what kinds of lessons are useful? Philos Trans R Soc A Math Phys Eng Sci 1893;2009(367):1571–85.
[6] Bhushan B, Jung YC. Natural and biomimetic artificial surfaces for superhydrophobicity, self-cleaning, low adhesion, and drag reduction. Prog Mater Sci 2011;56(1):1–108.
[7] Hargroves K, Smith M. Innovation inspired by nature: Biomimicry. ECOS 2006;129:27–9.
[8] Wang L, Song J, Ortiz C, Boyce MC. Anisotropic design of a multilayered biological exoskeleton. J Mater Res 2009;24(12):3477–94.
[9] Yang W, Chen IH, Gludovatz B, Zimmermann EA, Ritchie RO, Meyers MA. Natural flexible dermal armor. Adv Mater 2013;25(1):31–48.
[10] Kardong KV. Vertebrates: comparative anatomy function evolution. Boston (MA): McGraw-Hill; 2006. p. 782.
[11] Sire JY, Huysseune ANN. Formation of dermal skeletal and dental tissues in fish: a comparative and evolutionary approach. Biol Rev 2003;78(2):219–49.
[12] Raschi W, Tabit C. Functional aspects of placoid scales: a review and update. Mar Freshw Res 1992;43(1):123–47.
[13] Jandt KD. Biological materials: fishing for compliance. Nat Mater 2008;7(9):692–3.
[14] Bruet BJ, Song J, Boyce MC, Ortiz C. Materials design principles of ancient fish armour. Nat Mater 2008;7(9):748–56.
[15] Chen PY, Schirer J, Simpson A, Nay R, Lin YS, Yang W, et al. Predation versus protection: fish teeth and scales evaluated by nanoindentation. J Mater Res 2012;27(1):100.
[16] Allison PG, Chandler MQ, Rodriguez RI, Williams BA, Moser RD, Weiss Jr CA, et al. Mechanical properties and structure of the biological multilayered material system, *Atractosteus spatula* scales. Acta Biomater 2013;9(2):5289–96.
[17] Yang W, Gludovatz B, Zimmermann EA, Bale HA, Ritchie RO, Meyers MA. Structure and fracture resistance of alligator gar (*Atractosteus spatula*) armored fish scales. Acta Biomater 2013;9(4):5876–89.
[18] Arola D, Bajaj D, Ivancik J, Majd H, Zhang D. Fatigue of biomaterials. Hard tissues. Int J Fatigue 2010;32(9):1400–12.
[19] Marino Cugno Garrano A, La Rosa G, Zhang D, Niu LN, Tay FR, Majd H, et al. On the mechanical behavior of scales from *Cyprinus carpio*. J Mech Behav Biomed Mater 2012;7:17–29.
[20] Ikoma T, Kobayashi H, Tanaka J, Walsh D, Mann S. Microstructure, mechanical, and biomimetic properties of fish scales from *Pagrus major*. J Struct Biol 2003;142(3):327–33.
[21] Liu WT, Zhang Y, Li GY, Miao YQ, Wu XH. Structure and composition of teleost scales from snakehead *Channa argus* (Cantor) (Perciformes: Channidae). J Fish Biol 2008;72(4):1055–67.
[22] Lin YS, Wei CT, Olevsky EA, Meyers MA. Mechanical properties and the laminate structure of *Arapaima gigas* scales. J Mech Behav Biomed Mater 2011;4(7):1145–56.
[23] Bigi A, Burghammer M, Falconi R, Koch MH, Panzavolta S, Riekel C. Twisted plywood pattern of collagen fibrils in teleost scales: an X-ray diffraction investigation. J Struct Biol 2001;136(2):137–43.
[24] Zhu D, Ortega CF, Motamedi R, Szewciw L, Vernerey F, Barthelat F. Structure and mechanical performance of a "modern" fish scale. Adv Eng Mater 2012;14(4):B185–94.
[25] Yang W, Sherman V, Gludovatz B, Mackey M, Zimmermann EA, Chang EH, et al. Protective role of *Arapaima gigas* fish scales: structure and mechanical behavior. Acta Biomater 2014;10(08):3599–614.
[26] Torres FG, Troncoso OP, Nakamatsu J, Grande CJ, Gomez CM. Characterization of the nanocomposite laminate structure occurring in fish scales from *Arapaima Gigas*. Mater Sci Eng, C 2008;28(8):1276–83.
[27] Zhu D, Szewciw L, Vernerey F, Barthelat F. Puncture resistance of the scaled skin from striped bass: collective mechanisms and inspiration for new flexible armor designs. J Mech Behav Biomed Mater 2013;24:30–40.
[28] Currey JD. The design of mineralized hard tissues for their mechanical functions. J Exp Biol 1999;202(23):3285–94.
[29] ASTM, in D-1938. Standard test method for tear-propagation resistance (trouser tear) of plastic film and thin sheeting by a single-tear method (2008).
[30] Rivlin RS, Thomas AG. Rupture of rubber. I. Characteristic energy for tearing. J Polym Sci 1953;10(3):291–318.
[31] Griffith AA. VI. The Phenomena of Rupture and F low in Solids. Phil Trans R Soc (Lond) A 1920;221:163–98.
[32] Chen L. Tear energy of natural rubber under dynamic loading [doctoral dissertation]. University of Akron; 2008.
[33] Gdoutos EE, Daniel IM, Schubel P. Fracture mechanics of rubber. Facta Univ Ser Mech Automatic Control Robotics 2003;3(13):497–510.

[34] Zulkifli R, Azhari CH, Nor MJM, Oshkovr S. The effect of plies and processing time on mode I and mode III fracture properties of woven silk fibre/polyester composites. In: Proceedings of the 4th WSEAS international conference on applied and theoretical mechanics (2008).
[35] Ahagon ATA, Gent AN, Kim HJ, Kumagai Y. Fracture energy of elastomers in mode I (cleavage) and mode III (lateral shear). Rubber Chem Technol 1975;48(5):896–901.
[36] Ahagon A, Gent AN. Threshold fracture energies for elastomers. J Polym Sci Polym Phys Ed 1975;13(10):1903–11.
[37] Mouzakis DE, Gahleitner M, Karger-Kocsis J. Toughness assessment of elastomeric polypropylene (ELPP) by the essential work of the fracture method. J Appl Polym Sci 1998;70(5):873–81.
[38] Le Guellec D, Morvan-Dubois G, Sire JY. Skin development in bony fish with particular emphasis on collagen deposition in the dermis of the zebrafish (*Danio rerio*). Int J Dev Biol 2004;48:217–32.
[39] Sire JY, Akimenko MA. Scale development in fish: a review, with description of sonic hedgehog (shh) expression in the zebrafish (*Danio rerio*). Int J Dev Biol 2005;48:233–48.
[40] Browning A, Ortiz C, Boyce MC. Mechanics of composite elasmoid fish scale assemblies and their bioinspired analogues. J Mech Behav Biomed Mater 2013;19:75–86.
[41] Chintapalli RK, Mirkhalaf M, Dastjerdi AK, Barthelat F. Fabrication, testing and modeling of a new flexible armor inspired from natural fish scales and osteoderms. Bioinspir Biomim 2014;9(3):036005.
[42] Sperling LH. Introduction to physical polymer science. John Wiley & Sons; 2005 [Chapter 8].
[43] Sarti B, Scandola M. Viscoelastic and thermal properties of collagen/poly(vinyl alcohol) blends. Biomaterials 1995;16(10):785–92.
[44] Chien JCW. Solid-state characterization of the structure and property of collagen. J Macromol Sci Rev Macromol Chem 1975;C12(1):1.
[45] Maccagno TM, Knott JF. The fracture behaviour of PMMA in mixed modes I and II. Eng Fract Mech 1989;34(1):65–86.
[46] Ramachandran GN, Chandrasekharan R. Interchain hydrogen bonds via bound water molecules in the collagen triple helix. Biopolymers 1968;6(11):1649–58.
[47] Vernerey FJ, Barthelat F. On the mechanics of fishscale structures. Int J Solids Struct 2010;47(17):2268–75.
[48] Park EH, Lee SH. Scale growth and squamation chronology for the laboratory-reared hermaphroditic fish *Rivulus marmoratus* (Cyprinodontidae). Jap J Ichthyol 1988;34(4):476–82.
[49] Tench D, White J. Enhanced tensile strength for electrodeposited nickel-copper multilayer composites. Metall Trans A 1984;15(11):2039–40.
[50] LeBaron PC, Wang Z, Pinnavaia TJ. Polymer-layered silicate nanocomposites: an overview. Appl Clay Sci 1999;15(1):11–29.
[51] Zhang Y, Pan C. Measurements of mechanical properties and number of layers of graphene from nano-indentation. Diam Relat Mater 2012;24:1–5.
[52] Zimmermann EA, Gludovatz B, Schaible E, Dave NK, Yang W, Meyers MA, et al. Mechanical adaptability of the Bouligand-type structure in natural dermal armour. Nat Commun 2013;4.
[53] Dastjerdi AK, Barthelat F. Teleost fish scales amongst the toughest collagenous materials. J Mech Behav Biomed Mater 2014 [in press], pii: S1751-6161(14)00309-9.
[54] Bereiter-Hahn J, Zylberberg L. Regeneration of teleost fish scale. Comp Biochem Physiol A Physiol 1993;105(4):625–41.
[55] de Vrieze E, Sharif F, Metz JR, Flik G, Richardson MK. Matrix metalloproteinases in osteoclasts of ontogenetic and regenerating zebrafish scales. Bone 2011;48(4):704–12.
[56] Ohira Y, Shimizu M, Ura K, Takagi Y. Scale regeneration and calcification in goldfish *Carassius auratus*: quantitative and morphological processes. Fish Sci 2007;73(1):46–54.
[57] Barthelat F, Mirkhalaf M. The quest for stiff, strong and tough hybrid materials: an exhaustive exploration. J R Soc Interface 2013;10(89):20130711.
[58] Barthelat F. Science and engineering of natural materials: merging structure and materials". J Mech Behav Biomed Mater 2013;19:1.